Ligand oligomerization state controls Tie2 receptor trafficking and angiopoietin-2-specific responses

Riikka Pietilä[1], Marjut Nätynki[1], Tuomas Tammela[2], Jaakko Kangas[1], Kristina H. Pulkki[2], Nisha Limaye[3], Miikka Vikkula[3], Gou Young Koh[4], Pipsa Saharinen[2], Kari Alitalo[2] and Lauri Eklund[1,*]

[1]Oulu Center for Cell-Matrix Research, Biocenter Oulu and Department of Medical Biochemistry and Molecular Biology, University of Oulu, FI-90014 Oulu, Finland
[2]Molecular Cancer Biology Laboratory, Biomedicum Helsinki, University of Helsinki, Haartmaninkatu 8, 00290 Helsinki, Finland
[3]de Duve Institute, Université Catholique de Louvain, Avenue Hippocrate 75, B1.75.10, B-1200 Brussels, Belgium
[4]Biomedical Center and Department of Biological Sciences, Korea Advanced Institute of Science and Technology, Daejeon 305-701, Korea
*Author for correspondence (lauri.eklund@oulu.fi)

Accepted 26 December 2011
Journal of Cell Science 125, 2212–2223

doi: 10.1242/jcs.098020

Summary

Angiopoietin 1 (Ang1) is an activating ligand for the endothelial receptor tyrosine kinase Tie2, whereas Ang2 acts as a context-dependent agonist or antagonist that has a destabilizing effect on the vasculature. The molecular mechanisms responsible for the versatile functions of Ang2 are poorly understood. We show here that Ang2, but not Ang1, induces Tie2 translocation to the specific cell–matrix contact sites located at the distal end of focal adhesions. The Ang2-specific Tie2 translocation was associated with distinct Tie2 activation and downstream signals which differed from those of Ang1, and led to impaired cell motility and weak cell–matrix adhesion. We demonstrate that the different oligomeric or multimeric forms of the angiopoietins induce distinct patterns of Tie2 trafficking; the lower oligomerization state of native Ang2 was crucial for the Ang2-specific Tie2 redistribution, whereas multimeric structures of Ang1 and Ang2 induced similar responses. The Ang2-specific Tie2 trafficking to cell–matrix contacts was also dependent on the cell substratum, α2β1-integrin-containing cell–matrix adhesion sites and intact microtubules. Our data indicate that the different subcellular trafficking of Tie2–Ang2 and Tie2–Ang1 complexes generates ligand-specific responses in the angiopoietin–Tie signaling pathway, including modulation of cell–matrix interactions.

Key words: Angiopoietin, Cell–matrix adhesion, Endothelial cell, Tie2, Trafficking

Introduction

Angiopoietin growth factors (Ang1–Ang4) and their Tie receptors (Tie1 and Tie2) are essential for vascular remodeling and vessel integrity (Augustin et al., 2009). Unlike other receptor tyrosine kinases, Tie2 shows unique, Ang1-mediated compartmentalization in endothelial cells (ECs) (Fukuhara et al., 2008; Saharinen et al., 2008), which is affected by the Tie2 mutations that result in human venous malformations (Limaye et al., 2009). Ang2 was initially identified as a natural antagonist of Tie2, counteracting Ang1-induced activation (Maisonpierre et al., 1997), but a number of subsequent studies have indicated that Ang2 can also function as a context-dependent Tie2 agonist. Although Ang2 signaling is poorly understood, it is known that Tie2 activation by Ang2 is dependent on the cellular context (Maisonpierre et al., 1997), Ang2 dose (Kim et al., 2000), exposure time (Teichert-Kuliszewska et al., 2001), oligomerization state (Kim et al., 2009) and cellular source (Daly et al., 2006). In mice, Ang1 and Ang2 show both opposite (Maisonpierre et al., 1997; Reiss et al., 2007) and redundant activities (Gale et al., 2002). Ang2 deletion leads to dysmorphogenesis of retinal blood vessels and lymphatic vessel defects (Gale et al., 2002). The lymphatic phenotype was rescued by substitution of *Ang1* cDNA for the *Ang2* locus, indicating that the angiopoietins have redundant roles in lymphatic development. By contrast, the Ang2-overexpression and Ang1-deletion phenotypes in mouse embryos were similar (Maisonpierre et al., 1997), indicating that Ang2 acts as an antagonist of Tie2 activation (Reiss et al., 2007).

These observations raise fundamental mechanistic questions regarding the versatile effects of Ang2, which we investigated in the work reported here. Previous studies have indicated that the functions of Tie2 depend on its subcellular localization (Fukuhara et al., 2008; Saharinen et al., 2008). Here we investigated whether the angiopoietin ligands induce differential subcellular sorting of the Tie2 receptors. We show that the lower oligomerization state of Ang2 in comparison with Ang1 is crucial for the Ang2-specific redistribution of Tie2. This mechanism determines Ang2-specific Tie2 translocation to endothelial-cell–matrix contacts on collagen substratum. The spatiotemporal regulation of Tie2 localization and activation might help to explain the versatile effects of Ang2.

Results

Ang2- and substrate-specific Tie2 translocation to cell–matrix contacts

To study the effects of Ang2 on cell–matrix contacts, we used freshly plated, actively spreading cells where extensive formation and remodeling of cell–matrix adhesion sites occurs. This model also allowed us to study spontaneous cell motility after the initial adhesion and spreading phases (supplementary material Movie 1). To study Tie2 receptor redistribution upon ligand binding ECs were fixed and Tie2 was visualized by immunostaining. After

Ang2 stimulation, Tie2 was observed in clusters that resembled classical cell–matrix adhesion sites (Fig. 1A,B). These were not typical focal adhesions (FAs), however, nor focal complexes, as shown by the lack of colocalization of vinculin (Fig. 1B), paxillin, β1 integrin, phosphotyrosine, Crk and actin stress fibers (supplementary material Fig. S1A–E). Instead, the Tie2 clusters were located adjacent to the distal ends of the FAs.

The close association between the Tie2 and FAs suggested that the Tie2–Ang2 clusters were localized to the basal cell surface. This was confirmed by staining de-roofed cells (Feltkamp et al., 1991) which lack cytoplasmic organelles (Fig. 1C,D), and by total internal reflection fluorescence (TIRF) microscopy (Fig. 1E–G), which specifically visualizes fluorochromes located within ~150 nm of the cell substratum (Axelrod, 2001). By contrast, Ang1 did not induce Tie2 translocation to the distal ends of the FAs, indicating ligand specificity (Fig. 1G). The Tie2–Ang2 cell–matrix contacts were formed in cells plated on collagen I (Col I). They occurred also on Col IV, but not on fibronectin (FN), poly-D-lysine or gelatin (supplementary material Fig. S1H–K).

To investigate Tie2 trafficking in living cells, HUVECs were transfected with Tie2–GFP. Time-lapse videomicroscopy indicated that the Ang2-induced Tie2–GFP foci were formed near the cell periphery and that they were static relative to the cell substratum (supplementary material Movie 2). In addition, the Tie2–Ang2 cell–matrix contacts increased in size in the more central regions of the cells owing to the tethering of new Tie2–GFP vesicles (supplementary material Movie 3). Few Tie2–GFP vesicles were present in the control cells, where Tie2–GFP was more homogeneously located (supplementary material Movie 4).

We previously reported that Ang1 induces Tie2 clusters located adjacent to the FAs (Saharinen et al., 2008). However, in contrast to the Tie2–Ang2 cell–matrix contacts, the Tie2–Ang1 clusters were located along the actin bundles proximal to the FAs (Fig. 1H). This indicated that the translocation of Tie2 ligand complexes to cell–matrix contacts is different for Ang1 and Ang2.

Ang2-specific Tie2 translocation is not dependent on Tie2 kinase activity

Ang1 readily activates Tie2, whereas Ang2 induces weak or no Tie2 phosphorylation in confluent ECs (Saharinen et al., 2008). To test the effect of Tie2 phosphorylation on its subcellular sorting, we plated HUVECs, or NIH3T3 fibroblasts transfected with wild-type Tie2 (Tie2-WT), kinase-negative (Tie2-KN), intracellularly deleted (Tie2-ΔIC), or hyperphosphorylated (Tie2-R915C) Tie2 on Col I (supplementary material Fig. S2). Following Ang2 stimulation, all these forms of Tie2 were translocated to the distal ends of the FAs, indicating that the translocation is not dependent on Tie2 phosphorylation or the Tie2 intracellular domain. Furthermore, lack of Tie2 kinase activity did not alter the Ang1-induced Tie2 redistribution, indicating that differences in Tie2 kinase activity are not responsible for differential Tie2 trafficking induced by Ang1 and Ang2 (supplementary material Fig. S2F). Translocation of Tie2–Ang2 also occurred in fibroblasts, indicating that it is independent of cell type. This result also ruled out the possibility that translocation of the mutant forms of Tie2 occurred by interaction with endogenous Tie2-WT or Tie1 in the ECs.

Low-order oligomers of native Ang2 induce Tie2 translocation to specific cell–matrix contacts

Native Ang2 exists predominantly in oligomeric forms, and in rare cases multimeric structures, whereas Ang1 regularly forms

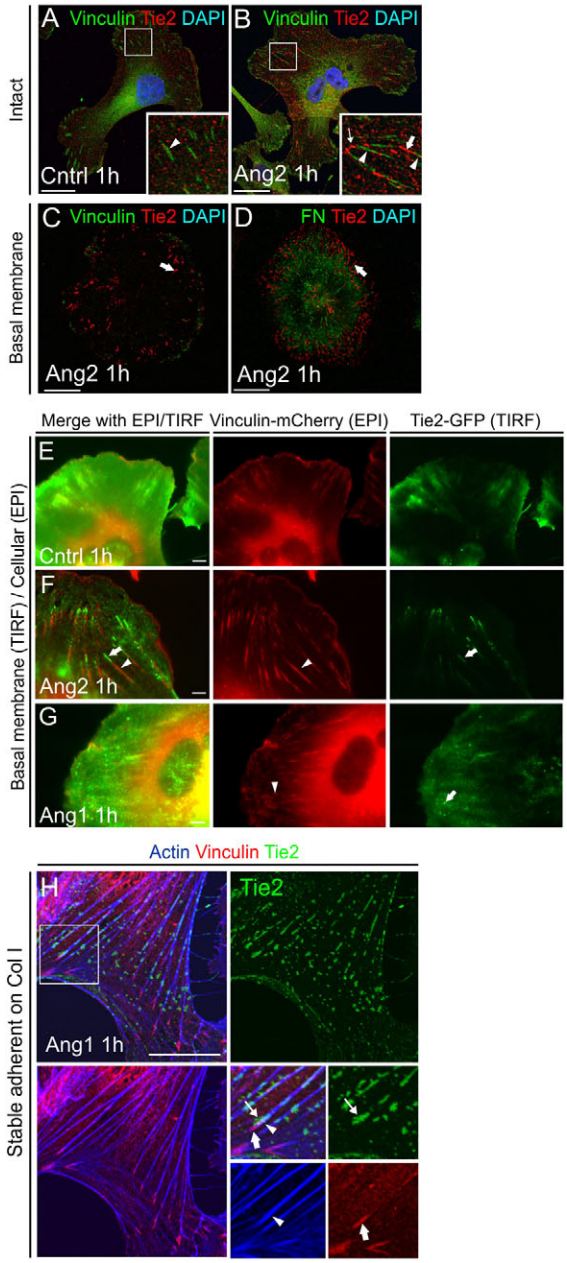

Fig. 1. Ang2 induces the translocation of Tie2 to cell–matrix contact sites located at the distal ends of FAs. (**A**,**B**) Non-transfected HUVECs were plated on Col I for 1 hour in the absence (A) or presence of Ang2 (B). FAs were stained using a vinculin antibody (A,B, arrowheads). Note that Ang2 induces Tie2 translocation to small foci (thin arrow) and to more elongated fiber-like structures (thick arrow) located at the distal ends of the FAs. (**C**,**D**) De-roofing of the cells removed apical plasma membrane and the cytoplasmic organelles, including the nucleus and the majority of vinculin (C), but shows Tie2 clusters (arrows) and cell matrix fibronectin (FN, green) attached to the substratum (D). (**E**–**G**) Tie2–GFP and mCherry–vinculin-transfected HUVECs were plated on Col I in the presence of the indicated ligands. GFP and mCherry were detected using epifluorescence (EPI), and GFP also using TIRF. Note that Ang2-induced, but not Ang1-induced, Tie2–GFP clusters (arrow) are associated with FAs (arrowhead) and are visible by TIRF, demonstrating proximity to the cell substratum. Tie2–GFP epifluorescence shows additional Tie2–GFP signals in vesicular structures. (**H**) Ang1-induced Tie2 clusters adjacent to the FAs in stable adherent cells on Col I. In contrast to the Tie2–Ang2 cell–matrix contacts, the Tie2–Ang1 clusters (thin arrow) are actin based (arrowhead) and located proximally to the FAs (thick arrow). Confocal microscopy images, boxed areas are magnified in inserts A–D,H. Scale bars: 20 μm (A–D,H) and 5 μm (E–G).

various larger complexes (Kim et al., 2005) (Fig. 2A,B). To study the effect of the ligand oligomerization state on Tie2 redistribution, Tie2-WT HUVECs were first plated in the presence of the pentameric Ang2 variant COMP-Ang2 (Kim et al., 2009). Both native Ang2 (supplementary material Movie 5) and COMP-Ang2 induced polarized Tie2 redistribution to the cell rear and sides (Fig. 2C). However, COMP-Ang2 did not induce Tie2 translocation to the specific cell–matrix contacts as observed with native Ang2 (Fig. 2E). In contrast to native angiopoietins, pentameric COMP-Ang2 and COMP-Ang1 had similar effects (Fig. 2D). To investigate further the importance of Ang2 oligomerization for Tie2 trafficking, we next pre-clustered Ang2 by treatment with an anti-Ang2 antibody (Fig. 2E,F and supplementary material Fig. S3A–G). A low ratio of clustering antibody (C-Ab) to Ang2 (in a ratio of ~1:50) allowed the formation of Tie2–Ang2 cell–matrix contacts. Interestingly, C-Ab–Ang2 was selectively associated with Tie2 at the cell rear and sides, but not in the cell–matrix contacts (supplementary material Fig. S3D). A high ratio of C-Ab to Ang2 (~8:1) prevented the formation of Tie2–Ang2 cell–matrix contacts (Fig. 2F) and induced a similar Tie2 redistribution to native multimeric Ang1 (supplementary material Fig. S3C). By contrast, further multimerization of Ang1 by C-Ab did not alter Tie2 translocation (supplementary material Fig. S3E,G) and monomeric Ang2 lacking the superclustering domain (supplementary material Fig. S4A, Ang2-ΔSCD) did not induce Tie2 receptor clustering. These experiments indicated that lower-order oligomeric Ang2 forms translocate Tie2 to cell–matrix contacts, whereas higher-order ligands polarize Tie2 into the retracting cell edges and cell–cell junctions.

The sizes of the higher-order multimeric Ang1 molecules have been estimated to be >200 nm (Kim et al., 2005). To investigate the dependence of ligand size on Tie2 trafficking, carboxylate-modified fluorescent beads of various sizes (20 nm to 1 μm) were added to the cells together with Ang1 or Ang2, and their association with the specific Tie2 compartments was analyzed (Fig. 2G–J and supplementary material Fig. S3H–M). The 20 nm spheres were found to be associated with the Tie2–Ang2 cell–matrix contacts more frequently than could be expected under conditions of random distribution (6.5±0.7% vs 2.8±0.1%, means ± s.e.m.; $P<0.001$) (Fig. 2I and supplementary material Fig. S3I). The larger spheres (100 nm and above) were excluded from the Tie2–Ang2 cell–matrix contacts, and accumulated

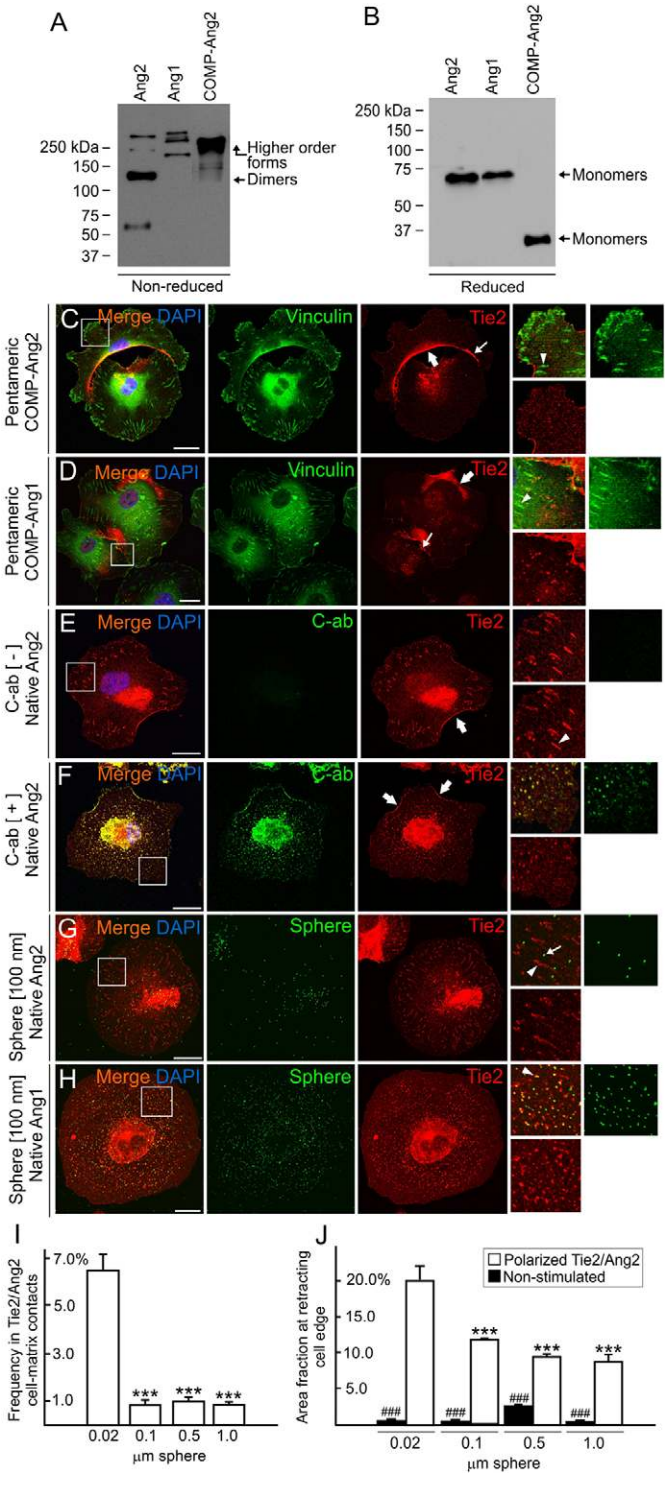

Fig. 2. A lower oligomerization state of native Ang2 is necessary for Tie2 translocation to specific cell–matrix contact sites. (**A**,**B**) SDS polyacrylamide gel electrophoresis of angiopoietins under non-reducing (A) and reducing (B, 5% β-mercaptoethanol) conditions. Recombinant Ang2 runs predominantly as disulfide-linked dimers, Ang1 forms larger complexes of various-sized, whereas COMP-Ang2 exists in penta- or hexameric forms. (**C**,**D**) Both COMP-Ang1 and COMP-Ang2 induce polarized Tie2 location in the cell rear (thick arrows) and at cell–cell junctions (thin arrows), but no Tie2 translocation to the distal ends of FAs (arrowheads). (**E**) Native Ang2 induced Tie2 translocation to specific cell–matrix contacts (arrowhead) and to the cell rear (thick arrow). (**F**) Antibody-clustered Ang2 (C-ab) fails to induce Tie2–Ang2 cell–matrix contacts, but colocalizes with Tie2 at the cell rear (thick arrows). (**G**–**J**) The effect of ligand size on Tie2 translocation was studied using carboxylate-modified fluorescent beads administered with the ligand. The association of spheres with specific Tie2 compartments was monitored in fixed cells after 1 hour of plating (G,H) and their frequencies at Tie2–Ang2 cell–matrix contacts (I) and at retracting cell edges (J) were calculated from digital images. (G) 100 nm spheres (thin arrow), which were excluded from the Tie2–Ang2 cell–matrix contacts (arrowhead) efficiently associated with Ang1-induced Tie2 compartments (H, arrowhead). (I) 20 nm spheres, but not larger ones, were associated with Tie2–Ang2 cell–matrix contacts whereas larger spheres accumulated with Tie2–Ang2 in the cell rear and sides (J). Confocal microscopy images, boxed areas are magnified on the right (C–H). Results are means ± s.e.m. for spheres. ***$P<0.001$, 20 nm vs larger spheres; $^{###}P<0.001$, sphere-covered area in non-stimulated vs Tie2–Ang2-containing retracting cell edges. Averages represent two to four separate experiments; 28–46 cells were included in each group. Scale bars: 20 μm.

instead with Tie2 in the cell rear and sides (Fig. 2J and supplementary material Fig. S3J–M). In contrast to Ang2, the larger spheres were found in all Tie2–Ang1 compartments (Fig. 2H). The strength of association of angiopoietins with the spheres did not differ (supplementary material Fig. S3N), suggesting that a lower oligomerization state of native Ang2 and the smaller size of resulting ligand–receptor complexes are crucial for the Ang2-specific redistribution of Tie2.

Ang2-specific Tie2 translocation is dependent on α2β1-integrin-containing FAs and intact microtubules

The requirement of a Col I or Col IV substrate for Ang2-induced Tie2 translocation suggested the involvement of the EC collagen receptors, the integrins α1β1 and α2β1 (Senger et al., 1997). Indeed, β1-integrin blocking antibody (Fig. 3B, AIIB2) and shRNA constructs directed against α2 integrin (Fig. 3C–E) inhibited the formation of the Tie2–Ang2 cell–matrix contacts (Fig. 3B). By contrast, polarized Tie2 translocation to the cell rear and sides occurred independently of the β1 and α2 integrins (Fig. 3B,D). The Tie2 clusters did not colocalize with β1 integrin (supplementary material Fig. S1B), suggesting a sequential mode of action rather than direct interactions between the integrins and Ang2-bound Tie2. This conclusion was consistent with the time-lapse experiments showing initial vinculin accumulation and subsequent Tie2–GFP translocation (supplementary material Movie 6). Formation of the Tie2–Ang2 cell–matrix contacts was also prevented in cells treated with methyl-β-cyclodextrin, which removes membrane cholesterol necessary for vinculin-positive FA formation (Marquez et al., 2008) (Fig. 3F), further supporting the importance of pre-formed FAs in Ang2–Tie2 translocation. By contrast, methyl-β-cyclodextrin did not prevent the polarization of Tie2 to the rear of the cells.

To investigate further the Tie2 trafficking induced by angiopoietins, we next studied the microtubules (MTs), known to be targeted to FAs and to serve as tracks for delivering cargo to cell–matrix adhesions (Kaverina et al., 1998; Wu et al., 2008). First, Ang2-induced Tie2 clusters were localized in the proximity of the MTs (supplementary material Fig. S1F). To investigate whether Tie2 translocation requires MTs, their polymerization was inhibited with nocodazole. This blocked the formation of MT

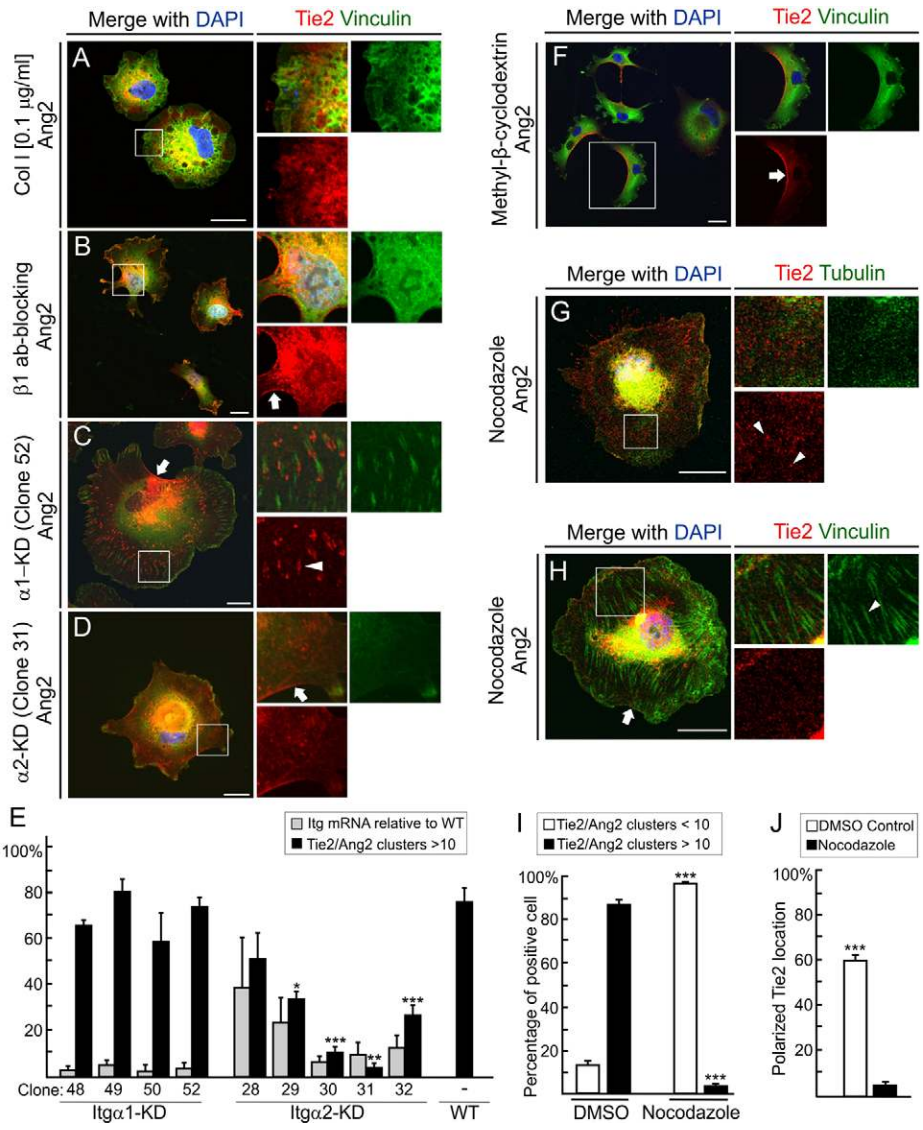

Fig. 3. Tie2 translocation to cell–matrix contacts is dependent on pre-formed FAs and intact microtubules. (**A**–**F**) The formation of vinculin-positive FAs was inhibited using either a low Col I concentration (A), β1-integrin-blocking antibodies (B), integrin RNAi (C–E) or cholesterol depletion (F). Note that the formation of Tie2–Ang2 cell–matrix contacts was inhibited, whereas Tie2 translocation to the cell rear and sides occurs (B–F, thick arrows). (C–E) Four α1 and five α2 lentiviral shRNA constructs were used. α2 but not α1 integrin shRNAs prevented formation of Tie2–Ang2 cell–matrix contacts, clones 30 and 31 exhibiting the highest reduction of α2 integrin mRNAs and most efficient inhibition of the Tie2–Ang2 translocation. Black bars represent the percentage of the cells having more than ten Tie2–Ang2 cell–matrix contacts. Results are means ± s.e.m. and represent two experiments run in duplicate, at least 300 cells from each group were included. *$P<0.05$, **$P<0.01$, ***$P<0.001$, lentiviral transfected vs control cells (WT). (**G**) Nocodazole inhibition of MTs prevents Ang2-induced Tie2 translocation to the cell–matrix contacts. Arrowheads show randomly distributed punctuate Tie2 immunoreactivity. (**H**) Nocodazole inhibits the polarized localization of Tie2 to the cell edges (thick arrow), whereas FAs (arrowhead) are able to form. (**I**) More than ten Tie2–Ang2 clusters were found in 87.2±2.1% of the DMSO-treated control cells, but in only 3.4±1.1% of the nocodazole-treated cells. (**J**) Polarized localization of Tie2 to the cell rear and sides was found in response to Ang2 in 59.5±2.6% of the DMSO-treated control cells, and in 5.1±1.6% of the nocodazole-treated MT deficient cells. Means ± s.d. represent four to six separate experiments; 897 nocodazole-treated and 1255 control cells were included. Confocal microscopy images, boxed areas are magnified on the right. Scale bars: 20 μm.

networks, and also Ang2-induced Tie2 translocation to the cell–matrix contacts (Fig. 3G,I). Interestingly, nocodazole also inhibited the polarized localization of Tie2 to the cell rear, whereas vinculin-positive FAs were still formed (Fig. 3H,J). Collectively, the results suggest that the FAs serve as targets for the MT-dependent translocation of Tie2–Ang2 to cell–matrix contacts. This trafficking differs mechanistically from the polarized Tie2 redistribution to the cell rear induced by higher-order ligands, which was not influenced by integrin blocking or cholesterol depletion. MTs are also involved establishing cellular polarity (Watanabe et al., 2005), which might be required for polarized Tie2 location.

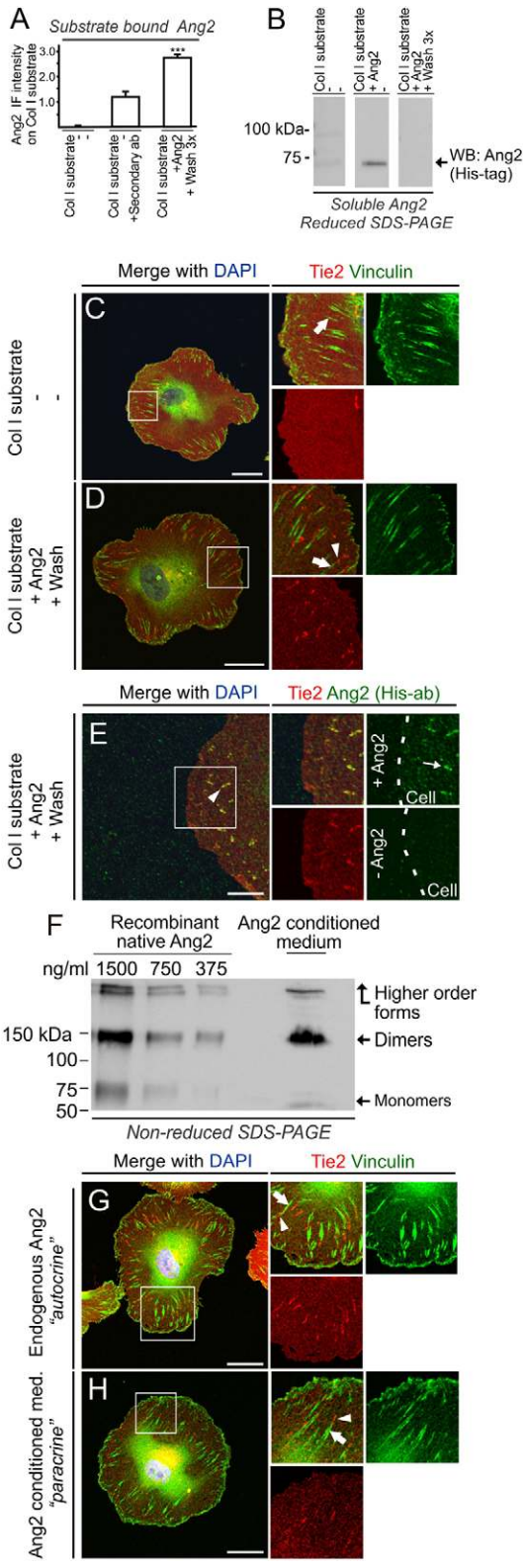

Both autocrine and substrate-bound Ang2 induce Tie2 translocation to cell–matrix contacts

The modes of Ang1 and Ang2 production differ markedly in vivo in that perivascular cells constitutively express Ang1, which activates endothelial Tie2 in a paracrine manner, whereas Ang2 is stored in EC-specific vesicles called Weibel–Palade bodies and is secreted locally by activated ECs on the apical (luminal) and abluminal (extracellular matrix) sides (Sporn et al., 1989; Fiedler et al., 2004). To test whether matrix-bound Ang2 is able to induce Tie2 redistribution to specific cell–matrix contacts, Tie2-WT HUVECs were plated on a Col-I–Ang2 substratum (Fig. 4A–E). This was sufficient to induce Tie2–Ang2 translocation to specific cell–matrix contacts (Fig. 4D). To compare the effects of autocrine and paracrine ligand presentation, Ang2-transfected HUVECs were plated on Col I in the presence of phorbol 12-myristate 13-acetate (PMA) to stimulate Ang2 release (Fiedler et al., 2004). Alternatively, HUVECs were plated on Col I in a conditioned medium containing Ang2 to mimic paracrine ligand presentation (Fig. 4F–H). Tie2 translocation to specific cell–matrix contacts occurred under both sets of conditions.

Substrate-bound Ang2 mediates weak cell adhesion and spreading

The above observations suggested that substrate-bound Ang2, like Ang1, might mediate the adhesion of Tie2-expressing cells as previously reported (Fukuhara et al., 2008; Saharinen et al., 2008). To test this, HUVECs and (Tie2-negative) fibroblasts were plated on immobilized angiopoietins. In contrast to Ang1, Ang2 mediated only weak cell adhesion (Fig. 5A,B). To test whether this resulted from an avidity effect as a result of a higher Ang1 multimerization state, the adhesion strength of Tie2-coated beads to angiopoietins was tested (supplementary material Fig.

Fig. 4. Col-I-bound and autocrine-released Ang2 induces Tie2 translocation to specific cell–matrix contacts. (**A**,**B**) Col-I-bound Ang2 substrate (Col I + Ang2 + Wash 3x) contained substrate-bound Ang2 (A; ***$P<0.001$ vs controls) and no detectable Ang2 in a soluble phase (B). (**C**–**E**) Tie2-WT HUVECs were plated for 1 hour on Col I in the absence of Ang2 or on Col I coated with Ang2, as indicated. Without Ang2, Tie2 was not aligned with vinculin (C, arrow). (D) Col I-linked Ang2 induced Tie2 translocation (arrowhead) to the distal ends of FAs (arrow). (E) Relatively even Ang2 staining was found on Col I outside the cell body. Instead, Ang2 (thin arrow) was clustered at Tie2-positive cell–matrix contacts (arrowhead), indicating uptake and redistribution of matrix-bound Ang2 with Tie2. Secondary antibody control (-Ang2, insert, bottom right panel) reveals no immunoreactivity. (**F**–**H**) To compare the paracrine and autocrine effects of Ang2 on the Tie2 distribution, Ang2-conditioned medium (F and H) and stimulated Ang2 release (G) were tested. (F) Western blot analysis of Ang2 conditioned medium revealed various sizes of Ang2 and a predominance of 150 kDa Ang2 dimers at a concentration of ~1000 ng/ml compared with serially diluted recombinant native Ang2. PMA-stimulated Ang2 release (G) and Ang2-conditioned medium (H) induced Tie2 translocation (arrowhead) to the distal ends of the FAs (arrow). Confocal microscopy images, boxed areas are magnified on the right. Scale bars: 20 µm (C,D,G,H) and 10 µm (E).

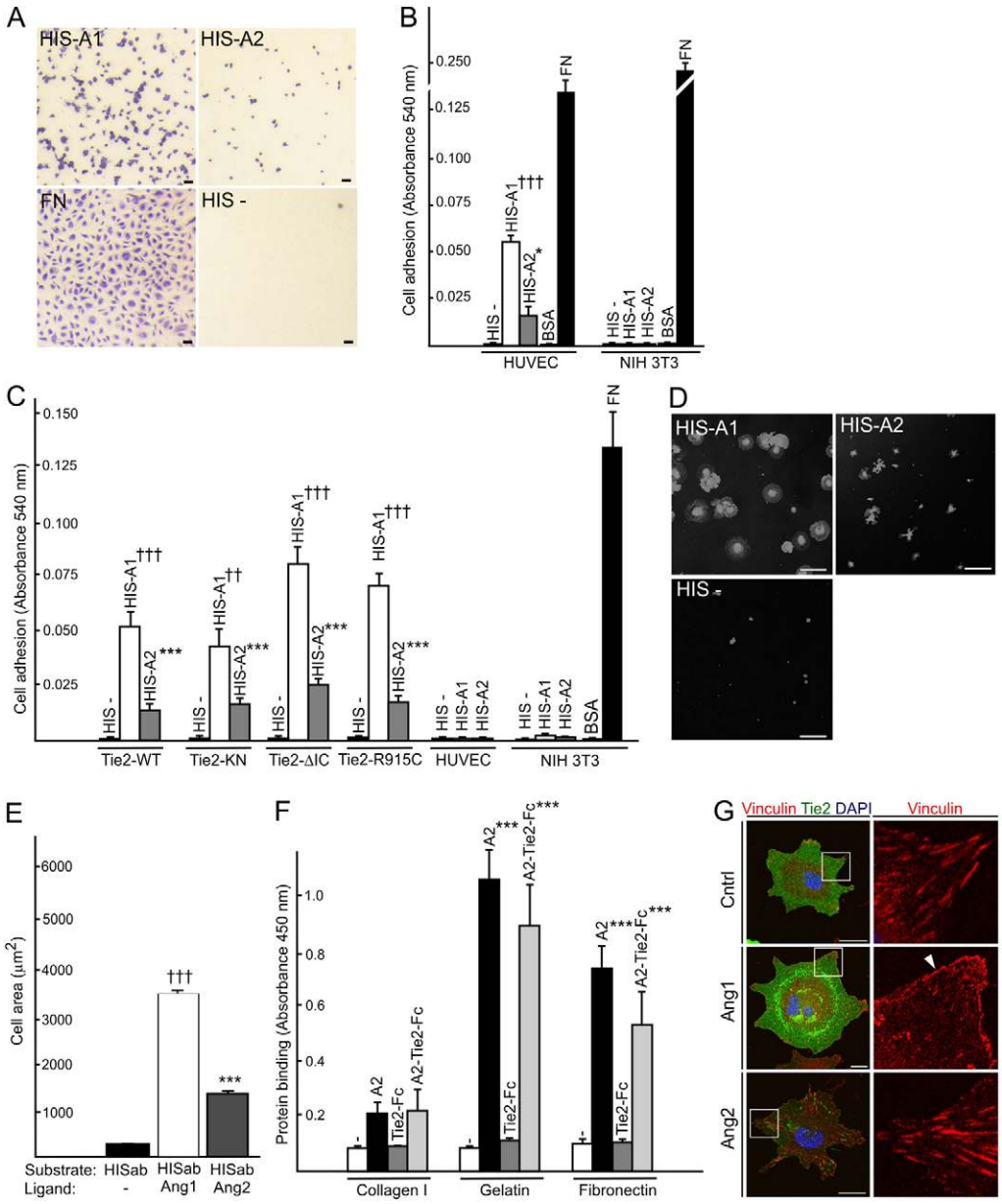

Fig. 5. Substrate-bound Ang2 provides weak support for cell adhesion and spreading. (**A**–**C**) Tie2–Ang2-mediated cell adhesion was tested using non-transfected HUVECs (HUVEC), Tie2-negative fibroblasts (NIH3T3) and retrovirally transfected HUVECs expressing either wild-type (WT), kinase-negative (KN), intracellular deletion (ΔIC), or constitutively active (R915C) Tie2 forms. Cells were allowed to adhere for 1 hour on immobilized His antibody (HIS-), His-antibody-linked Ang1 (HIS-A1) or -Ang2 (HIS-A2), fibronectin (FN) or albumin (BSA), washed, and then fixed and stained with crystal violet and photographed (A). The dye content was measured spectrophotometrically (B and C). (A,B) Under less-stringent washing conditions HUVECs adhered to immobilized Ang1, but Tie2-negative fibroblasts did not, whereas cell adhesion to Ang2 was significantly lower. (C) Non-transfected HUVECs were effectively removed under more stringent washing conditions, whereas overexpression of the Tie2 forms increased cell adhesion to angiopoietins. Tie2-negative fibroblasts adhered to FN only. (**D**) In a cell-spreading assay, Tie2-WT HUVECs were plated for 1 hour on coverslips coated as above. The cells were fixed, stained, photographed and the area measured on digital images. (**E**) A His–Ang2-coated substratum promoted the spreading of HUVECs compared with the negative control (HIS-), but the average cell area was significantly lower than that of the cells plated on His–Ang1. (**F**) The binding of Ang2 (A2), the extracellular domain of Tie2 (Tie2-Fc), and the Ang2–Tie2–Fc complex (A2-Tie2-Fc) to selected cell substrates was tested in a solid-phase binding assay. Ang2 binding to Col I was found to be low compared with that to gelatin and fibronectin. Tie2–Fc alone did not bind to the substrates tested. The ligand-negative control (HRP-conjugated secondary antibody) is indicated by a hyphen. B,C and E are means ± s.d. for three independent experiments run in triplicate. $^{\dagger\dagger\dagger}P<0.001$, $^{\dagger\dagger}P<0.01$ and $^{***}P<0.001$, $^{*}P<0.05$ for the comparison of cells on the His-Ang2 and His-Ang1 substrates, and His-Ang2 and His substrates, respectively. F shows means ± s.d. for four independent experiments run in duplicate. $^{***}P<0.001$ for the comparison of protein binding to Col I. (**G**) To compare the effects of angiopoietins on the formation of nascent cell–matrix adhesion sites at the cell periphery, Tie2-WT HUVECs were plated on Col I for 1 hour in the absence or presence of angiopoietins and stained. In the presence of Ang1, 85.4% of the cells ($n=157$) showed prominent vinculin staining at the cell periphery (arrowhead). This was observed in 5.0% of the unstimulated cells (Cntrl, $n=282$), and in 24.4% of the Ang2-stimulated cells ($n=160$). Scale bars: 100 μm (A,D) and 20 μm (G).

S3O). The Tie2 beads showed similar adhesion to Ang1 and Ang2, indicating that cellular component(s) are required to distinguish between substrate-bound Ang1 and Ang2. To investigate whether the adhesion correlates with Tie2 phosphorylation, which is more readily induced by Ang1 than by Ang2, cell adhesion to the angiopoietins was tested using HUVECs overexpressing Tie2-WT, Tie2-KN, Tie2-ΔIC or Tie2-R915C. Under stringent wash conditions, all forms of Tie2 mediated a stronger binding to Ang1 than to Ang2 (Fig. 5C). This indicated that the weaker cell adhesion to Ang2 was not dependent on the level of Tie2 phosphorylation in the adhering cells. The low potency of Ang2 to promote cell–matrix interactions through Tie2 was also evident in a cell-spreading assay on immobilized Ang2 (Fig. 5D,E). In addition, the strength of Ang2 binding to Col I was found to be markedly lower than that to gelatin or FN (Fig. 5F), consistent with the view that Ang2-bound Tie2 does not mediate strong cell–matrix interactions on Col I.

The Ang1 variant COMP-Ang1 promotes vinculin accumulation in the cell periphery, indicating increased formation of nascent cell–matrix adhesions (Fukuhara et al., 2008). Consistently, a prominent vinculin staining in cell periphery was observed in the presence of native Ang1 (Fig. 5G), but much less in the presence of Ang2. Instead, the Tie2–Ang2 clusters were primarily associated with elongated FAs when compared with non-stimulated HUVECs (4.3 ± 0.5 μm, $n=213$ vs 2.9 ± 0.6 μm, $n=1075$, mean ± s.d.; $P<0.001$).

Formation of Tie2–Ang2 cell–matrix contacts is dynamic and correlated with cell motility

Because the formation and turnover of FAs is necessary for efficient cell migration (Beningo et al., 2001), we next compared cell motility under conditions favoring Tie2–Ang2 translocation to cell–matrix contacts and in cells showing polarized Tie2 distribution (Fig. 6A–H). As controls, cell motility was studied on a gelatin substrate, which did not support the formation of the Tie2–Ang2 matrix contacts, and in HUVECs transfected with Tie2-ΔIC. An abundance of Tie2–Ang2 matrix contacts was associated with decreased cell motility in Tie2-WT HUVECs plated on Col I (Fig. 6A). This effect was not observed when the cells were plated on gelatin, nor in Tie2-ΔIC HUVECs plated on Col I (Fig. 6A). Although Tie2-ΔIC was translocated to cell–matrix contacts (supplementary material Fig. S2D), it had a dominant-negative effect on Tie2 phosphorylation and showed prominent translocation to the retraction fibers (supplementary material Fig. S4B), which contain disassembling adhesions at the cell rear, facilitating cell movements (Kirfel et al., 2004). This suggested that the lack of the Tie2 intracellular domain accelerates the disassembly of Tie2–Ang2 cell–matrix contacts, and that the decreased cell motility results from the Tie2–Ang2 cell–matrix contacts and is not a prerequisite for their formation.

In Tie2-WT HUVECs the Tie2–Ang2 cell–matrix contacts were mainly observed in the first hours after Ang2 stimulation (Fig. 6B). In addition, VEGF induced a shift from a stationary to a mobile cell phenotype (Fig. 6C–E) and polarized Tie2 distribution promoted intrinsic directionality (Petrie et al., 2009) in the mobile cells (Fig. 6F). To investigate cell motility after a prolonged ligand exposure, a modified 'wound-closure' migration assay was used (Fig. 6G,H). Tie2–Ang2 cell–matrix contacts were present after a short, but not prolonged, Ang2-stimulation (Fig. 6G), which correlated with cell motility on Col I (Fig. 6H). In this assay, Ang2 stimulated cell motility on gelatin, which is recognized by αvβ3 rather than α2β1 integrins in HUVECs (Rüegg et al., 1998; Starke et al., 2011). Collectively, the data suggested that Ang2-specific Tie2 translocation and inhibition of cell motility occurs early after Ang2 stimulation, and that VEGF and the ECM environment also modulate Ang2-induced functions. These observations prompted us to investigate whether native Ang2 (with ligand-specific Tie2 trafficking) and oligomerized or multimerized ligand forms (which act as native Ang1) have different effects on retinal angiogenesis in postnatal mouse. This has shown to be dependent on Ang2 and cannot be compensated with Ang1, suggesting that Ang2 antagonistic function is required (Gale et al., 2002). In this experiment, native angiopoietins and designed ligand forms were injected intravitreally into mouse eyes and the retinal vasculature was analyzed 24 hours later. Interestingly, native exogenous Ang2 increased the number of vessel branching points, but the other angiopoietin forms tested did not (Fig. 6I), suggesting that the Ang2-specific effects observed in cultured cells are related to vessel destabilization necessary for vascular sprouting.

Ang2 and Ang1 activate distinct Tie2 signaling responses in sparsely plated cells

We have previously shown that in confluent EC monolayers, which can mimic quiescent endothelium, an excess of Ang2 competed with Ang1 and decreased Tie2 tyrosine phosphorylation, indicating that Ang2 has an antagonistic function in cell–cell contacts (Saharinen et al., 2008). To investigate Tie2 signaling under conditions favoring Tie2 translocation to cell–matrix contacts, Tie2-WT HUVECs were plated on Col I in the presence or absence of angiopoietins and phosphorylation of Tie2 and downstream signaling mediators were analyzed by immunofluorescent staining and western blotting (Fig. 7). Antibodies against phosphorylated Tie2 showed staining in Tie2-containing vesicular structures in the presence of Ang2 (Fig. 7A–C). The colocalization of the Tie2 and phosphorylated Tie2 (Fig. 7B,C) or phosphorylated tyrosine (supplementary material Fig. S1C) was partial, suggesting that Tie2 activation by Ang2 depends on the subcellular compartment. The Ang2-induced Tie2 tyrosine phosphorylation was also evident in western blotting analysis (Fig. 7D). When the Tie2 downstream signaling mediators were analyzed by western blotting, increases in Akt and Erk1/2 phosphorylation were observed (Fig. 7E,F). However, the time course and extent of Tie2, Akt and Erk1/2 phosphorylation were different between Ang1 and Ang2, and this correlated with a differential subcellular localization of phosphorylated Tie2. The data suggested that in sparsely plated cells, which could mimic the angiogenic endothelium, Ang2 functions as a weak agonist and that subcellular compartmentalization events affect the ability of Ang2 to induce Tie2 phosphorylation.

Discussion

In this study, we have analyzed Ang2 ligand-specific Tie2 receptor trafficking and subcellular compartmentalization to cell–matrix contacts. Our findings reveal a novel sorting of receptor tyrosine kinase signaling complexes that is dependent on the ligand oligomerization state. Native Ang2 exists in different sizes and our data indicate that distinct ligand forms induce specific Tie2 receptor trafficking, subcellular compartmentalization and

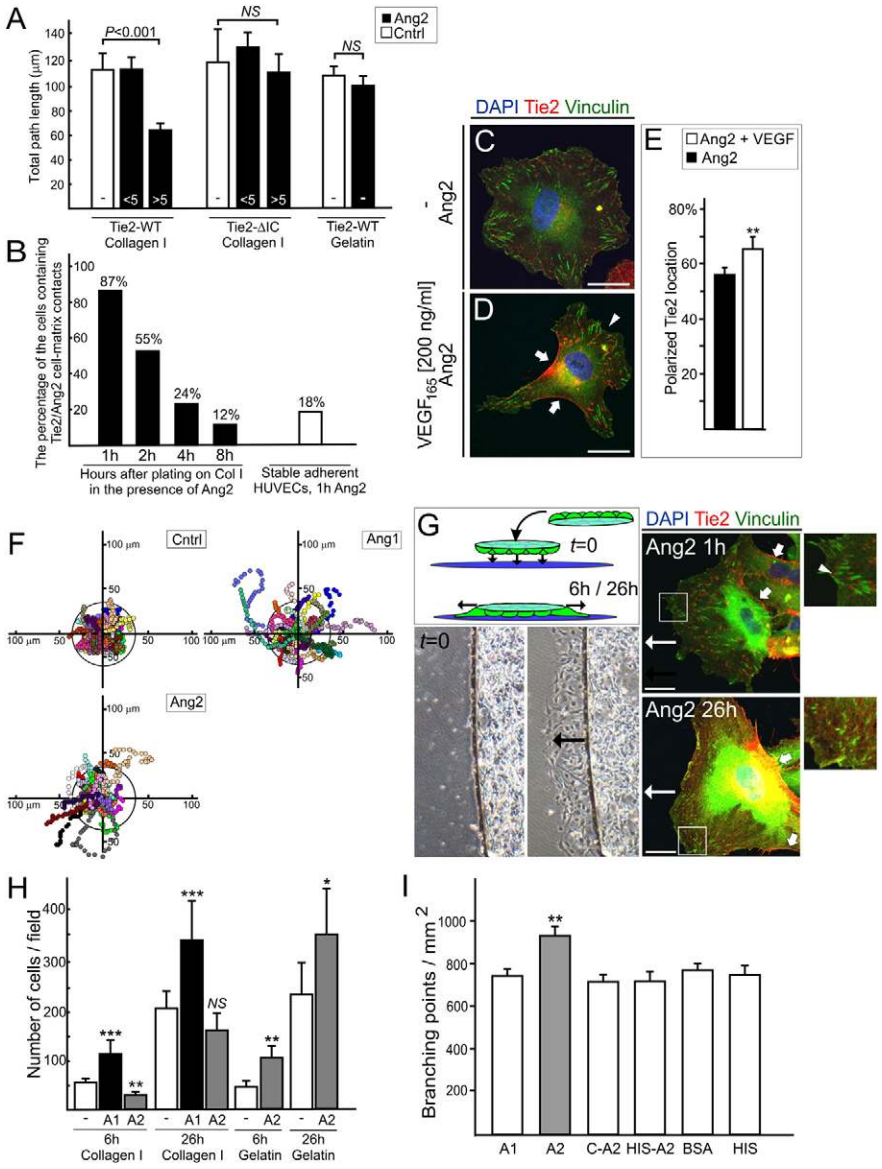

Fig. 6. Tie2–Ang2 cell–matrix contacts are dynamic structures correlated with cell motility. (**A**) HUVECs expressing either Tie2-WT or Tie2-ΔIC were plated on Col I or on gelatin and motility of individual cells was traced using time-lapse microscopy. Low motility in the Tie2-WT HUVECs correlated with a higher number of Tie2–Ang2 matrix contacts (>5 per cell). Ang2 had no effect on Tie2-ΔIC or on Tie2-WT HUVECs plated on gelatin. Bars represent means ± s.d.; *NS*, non-significant. Averages represent four to eight separate experiments, with 70–183 cells included in each group. (**B**) The percentage of the cells showing Tie2–Ang2 cell–matrix contacts as a function of time on Col I (n=367–1745 immunostained cells per time point). The Tie2–Ang2 cell–matrix contacts were found to be transient structures located under the actively protruding cell lamella in freshly plated spreading and stable adherent moving cells (white bar, Tie2-WT HUVECs allowed to adhere for 24 hours followed by Ang2 stimulation for 1 hour). (**C**–**E**) Tie2 polarization in HUVECs plated for 1 hour in the presence of Ang2 and VEGF. VEGF enhances a shift from a stationary (C, round cell with numerous Tie2–Ang2 cell–matrix contacts) to a mobile cell phenotype (D, protrusive lamella, arrowhead; polarized Tie2 location, arrows). $^{**}P<0.01$; means ± s.d. for two independent experiments run in duplicate; n=600 cells/group. (**F**) Scatter plots representing the motility of individual cells. Ang1-induced polarized Tie2 localization had no significant effect on the average total path length compared with non-stimulated controls (106.5±31.5 μm vs 101.2±23.7 μm, respectively; means ± s.d.; n=35). Instead, the polarized localization of Tie2 promoted directional movement, with 68% of cells showing a net path length greater than 40 μm (highlighted with a circle). In the non-stimulated controls and in Ang2 stimulated cells 10% and 26% of the cells migrated further than 40 μm, respectively. Each dot represents a cell location observed at two min intervals. The starting point of each track is superimposed at 0.0. (**G**,**H**) A modified 'wound-closure' migration assay. Cells migrated on the lower coverslip coated with selected substrates in the presence or absence (-) of Ang1 (A1) or Ang2 (A2) for the times indicated. (G) Schematic representation of assay principle (top panel) and phase-contrast images demonstrating migrating cells (lower panels, black arrow). Tie2–Ang2 cell–matrix contacts (arrowhead in magnified image on the right) were frequently found in the migration front after 1 hour but not after 26 hours Ang2 stimulation. By contrast, polarized Tie2 localization was persistent (thick arrows). Direction of movement is indicated by the thin arrows. (H) Quantification of the data. Note that Ang2 decreases the number of migrated cells on Col I when compared with non-stimulated controls after 6 hours, but not after 26 hours. By comparison, Ang1 induced cell migration on Col I and Ang2 stimulated migration on gelatin. Means ± s.e.m. for three independent experiments; n=12–36 microscopic fields/group. $^{***}P<0.001$, $^{**}P<0.01$, $^{*}P<0.05$ for the comparison of non-stimulated and ligand stimulated cells. (**I**) Effect of intravitreally injected angiopoietins on retinal vessel branching. Native Ang1 (A1), native Ang2 (A2), pentameric Ang2 (C-A2), His-antibody multimerized Ang2 (HIS-A2), and BSA and His antibody (HIS) controls were administered on postnatal day 4. The retinas were dissected and stained 24 hours later, and branching points in relation to the total area were calculated. Means ± s.e.m.; $^{**}P<0.01$ native Ang2 vs BSA. Averages represent four segments visualized from three to eight eyes per group.

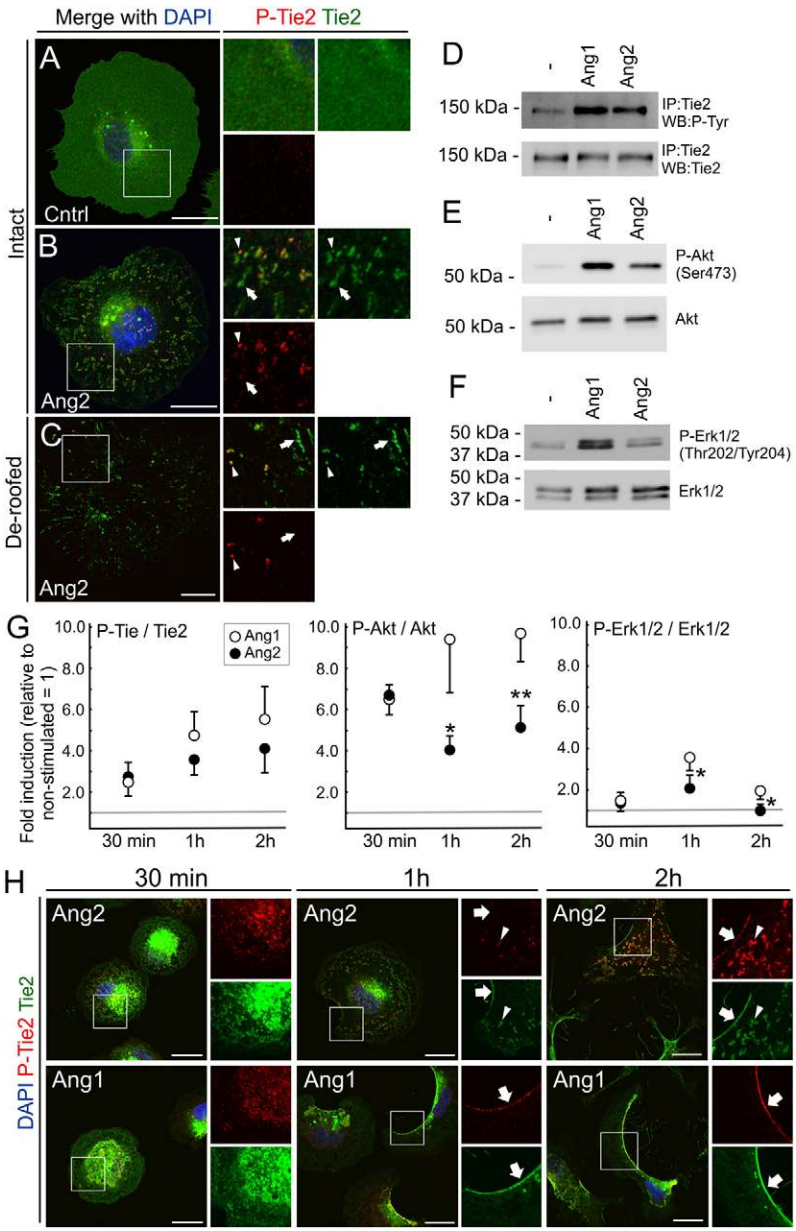

Fig. 7. Ang2 and Ang1 activate distinct Tie2 signaling responses in sparsely plated cells. (**A**–**F**) Tie2-WT HUVECs were plated on Col I for 1 hour in the absence (A), or presence of Ang2 (B,C), fixed and stained for total Tie2 (Tie2) and its phosphorylated form (P-Tie2) or analyzed by immunoblotting (D–F). (B) Phosphorylated Tie2 was detected in the vesicular structures (arrowhead). Not all compartments containing Tie2 were stained for phosphorylated Tie2 (arrow). (C) Both non-activated (arrow) and activated Tie2 (arrowhead) were found at the basal surface of de-roofed cells. (D) Tie2 was immunoprecipitated and analyzed by western blotting using anti-phosphotyrosine (P-Tyr) and anti-Tie2 antibodies. (E–F) Analysis of Akt and Erk1/2 by immunoblotting. (**G**,**H**) The western blot signal intensities were quantified and compared with phosphorylated Tie2 staining. After 1 hour (spreading) and 2 hours (spontaneously migrating cells), Ang1 induces a trend toward increased Tie2 tyrosine phosphorylation and higher phosphorylation of Akt and Erk1/2. $*P<0.05$, $**P<0.01$ Ang1 vs Ang2; means ± s.e.m. for four to seven independent experiments. At these time points, Ang1 and Ang2 resulted in distinct pattern of Tie2 subcellular activation; in the presence of Ang1 robust phosphorylated Tie2 staining was observed at the trailing edge of migrating cells (thick arrows), as previously reported (Saharinen et al., 2008). In this compartment, Ang2 induced little Tie2 phosphorylation (thick arrows). Instead, Ang2 induced more intense staining of phosphorylated Tie2 in distinct locations (arrowheads). Confocal microscopy images, boxed areas are magnified on the right. Scale bars: 20 μm.

cellular responses. These results should help to explain the versatile effects of Ang2 in angiogenesis.

Ang2 induced Tie2 translocation to specific cell–matrix contacts on Col I and Col IV substrates. Col IV is a major steady-state component of vascular basement membranes whereas Col I is exposed to the ECs in angiogenesis (Davis and Senger, 2005). The role of interstitial collagens in angiogenesis is not completely understood. Both stimulatory (Senger et al., 1997) and inhibitory functions (Mitola et al., 2006) have been reported, and fibrillar collagen matrix is remodeled especially in tumor angiogenesis (Weis and Cheresh, 2011). According to our substrate binding data, blocking antibody and mRNA interference experiments, the Ang2-specific Tie2 translocation was dependent on the collagen-binding integrin α2β1. In addition, Ang2 binding to Col I was weaker than to non-permissive substrates (gelatin, FN), which might be necessary for the Tie2 redistribution induced by substrate-bound Ang2.

In contrast to native Ang2-induced Tie2 translocation to specific cell–matrix contacts, higher-order and multimeric forms of Ang2 and Ang1, induced a polarized Tie2 location in the cell rear and sides. Such differential trafficking was not dependent on the Tie2 intracellular domain or kinase activity, indicating the importance of which ligand is bound. The angiopoietins consist of similar modular units assembled into oligomeric and multimeric structures of various sizes. Previous studies have indicated that the higher oligomeric forms (at least tetramers) are needed for Ang1-specific Tie2 binding and activation in the ECs (Davis et al., 2003; Kim et al., 2005). This is consistent with our data on the designed low oligomeric Ang1 forms that failed to induce Tie2 clustering in cells (not shown). In non-reducing SDS-PAGE, Ang2 ran predominantly as disulfide-linked dimers, with a few monomers and multimers, whereas Ang1 consisted of higher oligomeric and large heterogeneous multimers (Kim et al., 2009; Kim et al., 2005; Procopio et al., 1999). Rotary shadowing electron microscopy has revealed similar trimeric, tetrameric and

pentameric Ang1 and Ang2 structures (Kim et al., 2005; Davis et al., 2003). In this analysis, 50–55% of the Ang1 molecules formed large-sized multimers, whereas only 10–20% of Ang2 molecules were multimers (Kim et al., 2005). Based on our data, we propose that Tie2 trafficking is influenced by ligand valency and the size of the resulting ligand–receptor complexes. This conclusion is in line with the observation that there was a size-based cut-off for the cargo that associated with the Tie2–Ang2 cell–matrix contacts. This data is also consistent with the reported size-dependent subcellular distribution of internalized particles (Rejman et al., 2004; Jiang et al., 2008), and the effect of ligand valency on receptor clustering and intracellular trafficking (Tabas et al., 1991; Marsh et al., 1995; Mellman and Plutner, 1984; Jiang et al., 2008).

Matrix-bound Ang2 mediated relatively weak cell–matrix interactions and Tie2–Ang2 cell–matrix contacts were dynamic, occurring in the first hours after Ang2 stimulation. We also found that VEGF and distinct ECM that mimic angiogenic conditions enhanced a shift from a stationary to a mobile cell phenotype, and of the various angiopoietin forms, only native Ang2 increased the number of vessel branch points in retinal angiogenesis. The identified Ang2-specific functions might have a destabilizing effect on vessels that is necessary for sprouting angiogenesis. Furthermore, Ang2 might induce different effects depending on the stage of angiogenesis. In the vasculature, Tie2 is expressed in quiescent ECs and in stalk cells of vascular sprouts, but expression is lower in tip cells that are guided toward the angiogenic stimulus (Yana et al., 2007; del Toro et al., 2010). It is possible that angiopoietins do not control tip cells through Tie2, but regulate integrity and activation of quiescent vasculature and functions of stalk cells. Our data are in agreement with the recent observation that Ang2-blocking antibodies decreased retinal angiogenesis (Holopainen et al., 2012), and that Ang2 might also promote cell motility on substrates such as fibronectin (recognized by $\alpha5\beta1$ and $\alpha v\beta3$ integrins) (Rüegg et al., 1998; Mochizuki et al., 2002) and in wound-closure assays on culture dishes (Kim et al., 2009).

Ang2 behaves both as a weak agonist and an antagonistic ligand (Bogdanovic et al., 2006; Yuan et al., 2009). In sparsely plated cells, Ang2 induced Tie2 phosphorylation in distinct cellular compartments when compared with Ang1, whereas in cell–cell junctions of confluent cells Ang2 clusters Tie2 without inducing a significant Tie2 phosphorylation (Saharinen et al., 2008) and it destabilizes endothelial continuity (Holopainen et al., 2011). Molecular mechanisms regulating the agonistic versus antagonistic functions of Ang2 remain to be elucidated. However, subcellular sorting events that we describe might promote separation of Tie2–Ang2 complexes from plasma-membrane-proximal regulators. In addition, vesicular structures could represent a compartment where ligand concentration is relatively high, which has shown to promote Tie2 activation by Ang2 (Kim et al., 2000). Tie2 activation in distinct compartments might also lead to different signaling pathways, because the downstream effectors might be concentrated in specific subcellular domains (Hoeller et al., 2005).

Taken together, marked differences were found between the Tie2 translocation, subcellular activation and cellular effects induced by Ang1 and Ang2. Our data suggest that receptor trafficking and compartmentalization act as mechanisms for generating ligand-specific functions in the angiopoietin–Tie system. We also demonstrate that the extracellular matrix composition contributes to the versatile, context-dependent functions of Ang2. Thus the spatial and temporal compartmentalization of signal transduction pathways that regulate various signaling systems (Hoeller et al., 2005; Schutze et al., 2008; Omerovic and Prior, 2009) seem to determine the specificity of intracellular signaling and diverse cellular responses in the ECs.

Materials and Methods

Cell culture

HUVECs were cultured in M200 basal medium (Medium 200 with low-serum growth supplement, Cascade Biologics), supplemented with penicillin-streptomycin (Sigma-Aldrich) and 10% FBS (HyClone). NIH3T3 fibroblasts were maintained in DMEM (Gibco) supplemented with penicillin-streptomycin and 10% FBS. The packaging cell line 293-GPG VSV-G was maintained as described (Ory et al., 1996) and transfected for retrovirus production with Fugene 6 (Roche).

Immunofluorescence and image acquisition

Cells on substrate-coated coverslips were fixed using 4% paraformaldehyde in PBS (pH 7.2), permeabilized with 0.5% Triton X-100, blocked in 1% BSA in PBS, and incubated with primary antibodies overnight at 4℃, or for 1 hour at room temperature. The cells were incubated with secondary antibodies for 1 hour at room temperature. Confocal images were collected on an Olympus FluoView FV1000. TIRF images were captured on a Zeiss Observer Z1 microscope using an alpha Plan-Fluar $100\times/1.45$ NA oil-immersion objective and a Zeiss AxioCam MR3 camera (Carl Zeiss). Spinning-disk confocal images were acquired using an EM CCD camera (QuantEM: 512SC, Photometrics) integrated into a spinning-disk confocal scan head (CSU-X1, Yokogawa). The time-lapse phase-contrast and epifluorescence microscopy experiments were performed using an Olympus IX81 microscope and an F-View II camera (Olympus).

Generation of pre-clustered angiopoietin multimers

His-tagged angiopoietins were incubated for 1 hour with lower (2.1 μg/ml) or higher (105 μg/ml) ratios of anti-His antibody against angiopoietin (30 μg/ml). Clustered angiopoietins were used at a concentration 500 ng/ml. In the control experiments an equivalent amount of anti-His-antibody was used in the absence of any ligand.

Carboxylate-modified fluorescent microspheres

Spheres of sizes 20 nm, 100 nm, 500 nm and 1 μm (Molecular Probes, 505/515 nm excitation/emission maxima) were diluted 1:100 in 1% BSA in PBS and rotated for at least 2 hours at room temperature to prevent excessive ligand adsorption. After sonication for 3–5 minutes, the spheres, angiopoietins (final concentration 500 ng/ml) and cells (20,000) were mixed in M200 basal medium (total volume 350 μl) and plated for 1 hour followed by fixation. To test angiopoietin binding to the spheres, 96-well plates (MaxiSorp Surface, Nunc International) were coated with Ang1 or Ang2 (500 ng/ml) overnight at 4℃, washed three times with PBS and blocked with 1% heat-inactivated BSA in PBS for 2 hours. 100 nm beads (in M200 basal medium) were allowed to bind to the test substrates for 1 hour at 37℃ and washed twice with PBS, after which the fluorescence intensities were determined using a plate reader 515 nm.

Integrin function-blocking assays

Blocking antibody AIIB2 (1:50 dilution), was added to a cell suspension (200,000 cells/ml in M200 basal medium) for 30 minutes. The cells were allowed to spread on a Col I substrate in M200 basal medium containing Ang2 (500 ng/ml) and β1 integrin antibody (1:50 dilution) for 1 hour shRNA constructs are listed in supplementary material Table S1.

Cholesterol depletion

Cells were incubated for 30 minutes (37℃, 5% CO_2) in suspension (57,000 cells/ml in M200 basal medium) with 10 mM methyl-β-cyclodextrin. They were then plated on Col-I-coated coverslips in M200 basal medium in the presence or absence of Ang2 (500 ng/ml) for 1 hour.

Depolymerization of microtubules

Nocodazole diluted in dimethyl sulfoxide (DMSO) was added to the cell suspension (200,000 cells/ml in M200 basal medium) to a final concentration of 2.5 μg/ml for 45 minutes. The treated cells were then plated on Col-I-coated coverslips in M200 basal medium in the presence or absence of Ang2 (500 ng/ml) and nocodazole (0.7 μg/ml) for 1 hour. For the control cells, an equal amount of DMSO was used.

Preparation of Col-I-coated Ang2 substrate

Glass coverslips were coated with 40 µg/ml Col I overnight at 4℃, washed three times with PBS, blocked with heat-inactivated 1% BSA in PBS for 1 hour at room temperature and incubated with His-tagged Ang2 (500 ng/ml) in blocking buffer overnight at 4℃. Tie2-WT HUVECs (20,000 cells/well) were allowed to spread for 1 hour on coverslips washed three times with PBS, after which the cells were fixed and immunostained. The amount of soluble Ang2 was analyzed from the medium using anti-His antibody and western blotting after overnight incubation on Col I (Col I substrate+Ang2) and after three subsequent washes. Medium without Ang2 was used as a negative control. The amount of Ang2 bound to Col I was analyzed by immunofluorescence staining. The average fluorescence intensities of Col I- and Col I+Ang2-coated coverslips were measured using ImageJ software after three washes. DyLight 488 secondary antibody only was used as a negative control.

Ang2-conditioned medium

Conditioned medium (M200 basal medium) containing Ang2 was collected after overnight incubation of Ang2-transfected HUVECs and concentrated (~500 ng/ml) with 10 kDa Amicon Ultra-4 Centrifugal Filter Units (Millipore). Ang2-ΔSCD (lacking amino acid residues 1–86) was cloned into SignalpIg-plus vector, HEK293T cells were transfected using Fugene 6 (Roche), conditioned medium was collected after 48 hours, and concentrated (~20×). Media from native Ang2 and non-transfected HEK293T cells were used as controls.

Spreading assay on substrate-linked angiopoietins

Coverslips were coated with anti-His antibody (2.1 µg/ml) overnight at 4℃, followed by blocking with 1% heat-inactivated BSA-PBS for at least 2 hours. Recombinant His-tagged Ang1 or Ang2 (500 ng/ml in blocking buffer) were added and left overnight at 4℃. For negative controls, coverslips were coated with anti-His antibody only. 20,000 cells/well were allowed to spread for 1 hour in M200 basal medium before fixing and staining. The cell area was measured on digital images using ImageJ software.

Cell adhesion assay on substrate-linked angiopoietins

For the cell adhesion assays, 96-well plates (MaxiSorp Surface, Nunc International) were coated with 2.1 µg/ml anti-His antibody in PBS overnight at 4℃, followed by blocking with 1% heat-inactivated BSA-PBS for 2 hours and coating with His-tagged Ang1 or Ang2 (500 ng/ml in blocking buffer) overnight at 4℃. Wells were coated with anti-His antibody only or with fibronectin (20 µg/ml) for negative and positive controls, respectively. 25,000 cells/well were allowed to adhere for 1 hour in M200 basal medium, washed with PBS (once under less stringent washing conditions; four times under stringent conditions), fixed in cold methanol, stained with 0.05% crystal violet and photographed. To quantify cell adhesion, cells were lysed in 10 mM HEPES and 1% sodium deoxycholate and the amount of Crystal Violet was measured using a microplate spectrophotometer for absorbance at 540 nm and 405 nm to subtract the background.

Solid-phase binding assay

Coverslips were coated with Col I (40 µg/ml), fibronectin (20 µg/ml) or gelatin (0.1%) overnight at 4℃. Blocking was performed with 1% heat-inactivated BSA-PBS, followed by ligand incubation for 1 hour at 37℃ in M200 basal medium. His-tagged Ang2 (250 ng/ml), His-tagged Tie2-Fc (250 ng/ml), or a combination of Ang2 and Tie2-Fc (150 ng/ml and 100 ng/ml, respectively, mixed and pre-incubated for 15 minutes) were used as ligands. Washes were performed with 1×PBS (with Ca and Mg), 0.05% Tween 20, pH 7.4. Anti-His and HRP-conjugated antibodies in blocking buffer were used for 1 hour at room temperature. The coverslips were then relocated on a new plate, TMB X-tra substrate (Kem-En-Tec Diagnostics) was added for 13 minutes, the reaction was stopped with 0.2 M H_2SO_4, and absorbance was measured at 450 nm with a microplate spectrophotometer.

Adhesion of Tie2-coated beads to substrate-linked angiopoietins

To test binding of Tie2-coated beads to angiopoietins, 96-well plates (MaxiSorp Surface, Nunc International) were coated with Ang1 or Ang2 (500 ng/ml) overnight at 4℃, washed three times with PBS and blocked with 1% heat-inactivated BSA-PBS for 2 hours. BSA-coated wells and non-coated beads were used as negative controls. Protein G beads (2.8 µm, Invitrogen, 3 mg/ml) were incubated with Tie2-Fc (20 µg/ml) in PBS-0.1%Tween20 for 20 minutes with rotation, washed three times with PBS containing 0.1% Tween20, and resuspended in 200 µl PBS with 0.1% Tween20. Tie2-Fc-coated beads (10 µl in 100 µl PBS) were allowed to bind to the test substrates for 30 minutes, washed five times with PBS, and photographed. Area fraction of adhered beads was calculated from digital phase-contrast images using ImageJ software.

Time-lapse microscopy-based cell migration assay

To trace the motility of individual cells, the cells were plated on Col-I- or gelatin-coated glass-bottomed dishes in the presence or absence of angiopoietins (500 ng/ml), imaged every 30 seconds for 2 hours, and fixed and stained with antibodies against Tie2 and vinculin to visualize Tie2-positive compartments. Cell movement was tracked in ImageJ and the number of Tie2–Ang2 cell–matrix adhesion sites was calculated from the immunofluorescence images.

Modified 'wound-closure' migration assay

300,000 HUVECs were plated overnight on 14 mm coverslips, inverted on top of a 32 mm coverslip coated with either Col I or gelatin, gently pressed, and then incubated at 37℃, 5% CO_2 in M200 basal medium in the absence or presence of angiopoietins (500 ng/ml). Cells adhered to both upper and lower coverslips, resulting in a relatively firm construction and cell migration to the top of the lower coverslip. Migrated cells were photographed at twelve, three, six and nine o'clock positions followed by fixation and Tie2 staining.

Intravitreal injections

Mice at postnatal day 4 were injected (0.5 µl/eye) with Ang1, Ang2, Comp-Ang2 and multimerized Ang2 (His-tagged native Ang2 clustered with anti-His antibody), all at a concentration of 100 ng/µl in 0.2% BSA in PBS. Equivalent volumes of anti-His antibody (100 ng/µl) or 0.2% BSA in PBS were used as controls. The injections into the vitreous humor were performed under anesthesia with 75 mg/kg ketamine (Ketalar, Pfizer) and 10 mg/kg xylazine (Rompun, Bayer). Local anesthesia of the eye was performed with oxybuprocain eye drops (Oftan Obucain, Santen). Injections into the eye were carried out with a micromanipulator device (Joystick manipulator MN151, Narishige) using a 35G needle (NF35FBV-2, World Precision Instruments). The retinas were collected 24 hours after the injection, fixed in 4% PFA in PBS and the vasculature visualized with isolectin B4 staining (*Griffonia simplicifolica* lectin, Vector Laboratories). Quantitative analyses of branching points in relation to the total area were performed on digital images using the ImageJ software. Animal experimentation conformed to institutional guidelines.

DNA constructs, reagents and antibodies

A full list of all constructs reagents and antibodies can be found in supplementary material Table S1.

Statistical analysis

Cellular phenotypes were analyzed at least in three independent experiments (20,000 cells/coverslips) unless otherwise mentioned in the figure legends. Student's *t*-test was used to analyze differences between means.

Acknowledgements

We thank Jaana Träskelin for her excellent technical assistance, Antti Viklund for advice on computational image analysis, Sinikka Eskelinen for providing the vinculin cDNA, Naoki Mochizuki for DsRed-Crk, and Anita Lehtonen and other staff of the Meilahti Animal Facility at the University of Helsinki.

Funding

This work was supported by grants from the Academy of Finland [grant numbers 130446 to P.S. and 136880 to L.E.]; Finnish Centre of Excellence Program (2012–2017, L.E.); and the Louis Jeantet Foundation (K.A.).

Supplementary material available online at
http://jcs.biologists.org/lookup/suppl/doi:10.1242/jcs.098020/-/DC1

References

Augustin, H. G., Koh, G. Y., Thurston, G. and Alitalo, K. (2009). Control of vascular morphogenesis and homeostasis through the angiopoietin-Tie system. *Nat. Rev. Mol. Cell Biol.* **10**, 165-177.

Axelrod, D. (2001). Total internal reflection fluorescence microscopy in cell biology. *Traffic* **2**, 764-774.

Beningo, K. A., Dembo, M., Kaverina, I., Small, J. V. and Wang, Y. L. (2001). Nascent focal adhesions are responsible for the generation of strong propulsive forces in migrating fibroblasts. *J. Cell Biol.* **153**, 881-888.

Bogdanovic, E., Nguyen, V. P. and Dumont, D. J. (2006). Activation of Tie2 by angiopoietin-1 and angiopoietin-2 results in their release and receptor internalization. *J. Cell Sci.* **119**, 3551-3560.

Cho, C. H., Kammerer, R. A., Lee, H. J., Steinmetz, M. O., Ryu, Y. S., Lee, S. H., Yasunaga, K., Kim, K. T., Kim, I., Choi, H. H. et al. (2004). COMP-Ang1: a designed angiopoietin-1 variant with nonleaky angiogenic activity. *Proc. Natl. Acad. Sci. USA* **101**, 5547-5552.

Daly, C., Pasnikowski, E., Burova, E., Wong, V., Aldrich, T. H., Griffiths, J., Ioffe, E., Daly, T. J., Fandl, J. P., Papadopoulos, N. et al. (2006). Angiopoietin-2 functions as

an autocrine protective factor in stressed endothelial cells. *Proc. Natl. Acad. Sci. USA* **103**, 15491-15496.

Davis, G. E. and Senger, D. R. (2005). Endothelial extracellular matrix: biosynthesis, remodeling, and functions during vascular morphogenesis and neovessel stabilization. *Circ. Res.* **97**, 1093-1107.

Davis, S., Papadopoulos, N., Aldrich, T. H., Maisonpierre, P. C., Huang, T., Kovac, L., Xu, A., Leidich, R., Radziejewska, E., Rafique, A. et al. (2003). Angiopoietins have distinct modular domains essential for receptor binding, dimerization and superclustering. *Nat. Struct. Biol.* **10**, 38-44.

del Toro, R., Prahst, C., Mathivet, T., Siegfried, G., Kaminker, J. S., Larrivee, B., Breant, C., Duarte, A., Takakura, N., Fukamizu, A. et al. (2010). Identification and functional analysis of endothelial tip cell-enriched genes. *Blood* **116**, 4025-4033.

Feltkamp, C. A., Pijnenburg, M. A. and Roos, E. (1991). Organization of talin and vinculin in adhesion plaques of wet-cleaved chicken embryo fibroblasts. *J. Cell Sci.* **100**, 579-587.

Fiedler, U., Scharpfenecker, M., Koidl, S., Hegen, A., Grunow, V., Schmidt, J. M., Kriz, W., Thurston, G. and Augustin, H. G. (2004). The Tie-2 ligand angiopoietin-2 is stored in and rapidly released upon stimulation from endothelial cell Weibel-Palade bodies. *Blood* **103**, 4150-4156.

Fukuhara, S., Sako, K., Minami, T., Noda, K., Kim, H. Z., Kodama, T., Shibuya, M., Takakura, N., Koh, G. Y. and Mochizuki, N. (2008). Differential function of Tie2 at cell-cell contacts and cell-substratum contacts regulated by angiopoietin-1. *Nat. Cell Biol.* **10**, 513-526.

Gale, N. W., Thurston, G., Hackett, S. F., Renard, R., Wang, Q., McClain, J., Martin, C., Witte, C., Witte, M. H., Jackson, D. et al. (2002). Angiopoietin-2 is required for postnatal angiogenesis and lymphatic patterning, and only the latter role is rescued by Angiopoietin-1. *Dev. Cell* **3**, 411-423.

Hall, D. E., Reichardt, L. F., Crowley, E., Holley, B., Moezzi, H., Sonnenberg, A. and Damsky, C. H. (1990). The alpha 1/beta 1 and alpha 6/beta 1 integrin heterodimers mediate cell attachment to distinct sites on laminin. *J. Cell Biol.* **110**, 2175-2184.

Hoeller, D., Volarevic, S. and Dikic, I. (2005). Compartmentalization of growth factor receptor signalling. *Curr. Opin. Cell Biol.* **17**, 107-111.

Holopainen, T., Saharinen, P., D'Amico, G., Lampinen, A., Eklund, L., Sormunen, R., Anisimov, A., Zarkada, G., Lohela, M., Heloterä, H. et al. (2012). Effects of angiopoietin-2-blocking antibody on endothelial cell-cell junctions and lung metastasis. *J. Natl. Cancer Inst.* **104**, 461-475.

Huang, L., Turck, C. W., Rao, P. and Peters, K. G. (1995). GRB2 and SH-PTP2: potentially important endothelial signaling molecules downstream of the TEK/TIE2 receptor tyrosine kinase. *Oncogene* **11**, 2097-2103.

Jiang, W., Kim, B. Y., Rutka, J. T. and Chan, W. C. (2008). Nanoparticle-mediated cellular response is size-dependent. *Nat. Nanotechnol.* **3**, 145-150.

Kaverina, I., Rottner, K. and Small, J. V. (1998). Targeting, capture, and stabilization of microtubules at early focal adhesions. *J. Cell Biol.* **142**, 181-190.

Kim, H. Z., Jung, K., Kim, H. M., Cheng, Y. and Koh, G. Y. (2009). A designed angiopoietin-2 variant, pentameric COMP-Ang2, strongly activates Tie2 receptor and stimulates angiogenesis. *Biochim. Biophys. Acta* **1793**, 772-780.

Kim, I., Kim, J. H., Moon, S. O., Kwak, H. J., Kim, N. G. and Koh, G. Y. (2000). Angiopoietin-2 at high concentration can enhance endothelial cell survival through the phosphatidylinositol 3′-kinase/Akt signal transduction pathway. *Oncogene* **19**, 4549-4552.

Kim, K. T., Choi, H. H., Steinmetz, M. O., Maco, B., Kammerer, R. A., Ahn, S. Y., Kim, H. Z., Lee, G. M. and Koh, G. Y. (2005). Oligomerization and multimerization are critical for angiopoietin-1 to bind and phosphorylate Tie2. *J. Biol. Chem.* **280**, 20126-20131.

Kirfel, G., Rigort, A., Borm, B. and Herzog, V. (2004). Cell migration: mechanisms of rear detachment and the formation of migration tracks. *Eur. J. Cell Biol.* **83**, 717-724.

Limaye, N., Wouters, V., Uebelhoer, M., Tuominen, M., Wirkkala, R., Mulliken, J. B., Eklund, L., Boon, L. M. and Vikkula, M. (2009). Somatic mutations in angiopoietin receptor gene TEK cause solitary and multiple sporadic venous malformations. *Nat. Genet.* **41**, 118-124.

Maisonpierre, P. C., Suri, C., Jones, P. F., Bartunkova, S., Wiegand, S. J., Radziejewski, C., Compton, D., McClain, J., Aldrich, T. H., Papadopoulos, N. et al. (1997). Angiopoietin-2, a natural antagonist for Tie2 that disrupts in vivo angiogenesis. *Science* **277**, 55-60.

Márquez, M. G., Nieto, F. L., Fernández-Tome, M. C., Favale, N. O. and Sterin-Speziale, N. (2008). Membrane lipid composition plays a central role in the maintenance of epithelial cell adhesion to the extracellular matrix. *Lipids* **43**, 343-352.

Marsh, E. W., Leopold, P. L., Jones, N. L. and Maxfield, F. R. (1995). Oligomerized transferrin receptors are selectively retained by a lumenal sorting signal in a long-lived endocytic recycling compartment. *J. Cell Biol.* **129**, 1509-1522.

Mellman, I. and Plutner, H. (1984). Internalization and degradation of macrophage Fc receptors bound to polyvalent immune complexes. *J. Cell Biol.* **98**, 1170-1177.

Mitola, S., Brenchio, B., Piccinini, M., Tertoolen, L., Zammataro, L., Breier, G., Rinaudo, M. T., den Hertog, J., Arese, M. and Bussolino, F. (2006). Type I collagen limits VEGFR-2 signaling by a SHP2 protein-tyrosine phosphatase-dependent mechanism 1. *Circ. Res.* **98**, 45-54.

Mochizuki, Y., Nakamura, T., Kanetake, H. and Kanda, S. (2002). Angiopoietin 2 stimulates migration and tube-like structure formation of murine brain capillary endothelial cells through c-Fes and c-Fyn. *J. Cell Sci.* **115**, 175-183.

Nagashima, K., Endo, A., Ogita, H., Kawana, A., Yamagishi, A., Kitabatake, A., Matsuda, M. and Mochizuki, N. (2002). Adaptor protein Crk is required for ephrin-B1-induced membrane ruffling and focal complex assembly of human aortic endothelial cells. *Mol. Biol. Cell* **13**, 4231-4242.

Omerovic, J. and Prior, I. A. (2009). Compartmentalized signalling: Ras proteins and signalling nanoclusters. *FEBS J.* **276**, 1817-1825.

Ory, D. S., Neugeboren, B. A. and Mulligan, R. C. (1996). A stable human-derived packaging cell line for production of high titer retrovirus/vesicular stomatitis virus G pseudotypes. *Proc. Natl. Acad. Sci. USA* **93**, 11400-11406.

Petrie, R. J., Doyle, A. D. and Yamada, K. M. (2009). Random versus directionally persistent cell migration. *Nat. Rev. Mol. Cell Biol.* **10**, 538-549.

Popov, C., Radic, T., Haasters, F., Prall, W. C., Aszodi, A., Gullberg, D., Schieker, M. and Docheva, D. (2011). Integrins α2β1 and α11β1 regulate the survival of mesenchymal stem cells on collagen I. *Cell Death Dis.* **2**, e186.

Procopio, W. N., Pelavin, P. I., Lee, W. M. and Yeilding, N. M. (1999). Angiopoietin-1 and -2 coiled coil domains mediate distinct homo-oligomerization patterns, but fibrinogen-like domains mediate ligand activity. *J. Biol. Chem.* **274**, 30196-30201.

Reiss, Y., Droste, J., Heil, M., Tribulova, S., Schmidt, M. H., Schaper, W., Dumont, D. J. and Plate, K. H. (2007). Angiopoietin-2 impairs revascularization after limb ischemia. *Circ. Res.* **101**, 88-96.

Rejman, J., Oberle, V., Zuhorn, I. S. and Hoekstra, D. (2004). Size-dependent internalization of particles via the pathways of clathrin- and caveolae-mediated endocytosis. *Biochem. J.* **377**, 159-169.

Rüegg, C., Yilmaz, A., Bieler, G., Bamat, J., Chaubert, P. and Lejeune, F. J. (1998). Evidence for the involvement of endothelial cell integrin alphaVbeta3 in the disruption of the tumor vasculature induced by TNF and IFN-gamma. *Nat. Med.* **4**, 408-414.

Saharinen, P., Eklund, L., Miettinen, J., Wirkkala, R., Anisimov, A., Winderlich, M., Nottebaum, A., Vestweber, D., Deutsch, U., Koh, G. Y. et al. (2008). Angiopoietins assemble distinct Tie2 signalling complexes in endothelial cell-cell and cell-matrix contacts. *Nat. Cell Biol.* **10**, 527-537.

Schütze, S., Tchikov, V. and Schneider-Brachert, W. (2008). Regulation of TNFR1 and CD95 signalling by receptor compartmentalization. *Nat. Rev. Mol. Cell Biol.* **9**, 655-662.

Senger, D. R., Claffey, K. P., Benes, J. E., Perruzzi, C. A., Sergiou, A. P. and Detmar, M. (1997). Angiogenesis promoted by vascular endothelial growth factor: regulation through alpha1beta1 and alpha2beta1 integrins. *Proc. Natl. Acad. Sci. USA* **94**, 13612-13617.

Sporn, L. A., Marder, V. J. and Wagner, D. D. (1989). Differing polarity of the constitutive and regulated secretory pathways for von Willebrand factor in endothelial cells. *J. Cell Biol.* **108**, 1283-1289.

Starke, R. D., Ferraro, F., Paschalaki, K. E., Dryden, N. H., McKinnon, T. A., Sutton, R. E., Payne, E. M., Haskard, D. O., Hughes, A. D., Cutler, D. F. et al. (2011). Endothelial von Willebrand factor regulates angiogenesis. *Blood* **117**, 1071-1080.

Tabas, I., Myers, J. N., Innerarity, T. L., Xu, X. X., Arnold, K., Boyles, J. and Maxfield, F. R. (1991). The influence of particle size and multiple apoprotein E-receptor interactions on the endocytic targeting of beta-VLDL in mouse peritoneal macrophages. *J. Cell Biol.* **115**, 1547-1560.

Teichert-Kuliszewska, K., Maisonpierre, P. C., Jones, N., Campbell, A. I., Master, Z., Bendeck, M. P., Alitalo, K., Dumont, D. J., Yancopoulos, G. D. and Stewart, D. J. (2001). Biological action of angiopoietin-2 in a fibrin matrix model of angiogenesis is associated with activation of Tie2. *Cardiovasc. Res.* **49**, 659-670.

Watanabe, T., Noritake, J. and Kaibuchi, K. (2005). Regulation of microtubules in cell migration. *Trends Cell Biol.* **15**, 76-83.

Weis, S. M. and Cheresh, D. A. (2011). Tumor angiogenesis: molecular pathways and therapeutic targets. *Nat. Med.* **17**, 1359-1370.

Wu, X., Kodama, A. and Fuchs, E. (2008). ACF7 regulates cytoskeletal-focal adhesion dynamics and migration and has ATPase activity. *Cell* **135**, 137-148.

Yana, I., Sagara, H., Takaki, S., Takatsu, K., Nakamura, K., Nakao, K., Katsuki, M., Taniguchi, S., Aoki, T., Sato, H. et al. (2007). Crosstalk between neovessels and mural cells directs the site-specific expression of MT1-MMP to endothelial tip cells. *J. Cell Sci.* **120**, 1607-1614.

Yuan, H. T., Khankin, E. V., Karumanchi, S. A. and Parikh, S. M. (2009). Angiopoietin 2 is a partial agonist/antagonist of Tie2 signaling in the endothelium. *Mol. Cell. Biol.* **29**, 2011-2022.

Journal of Cell Science